

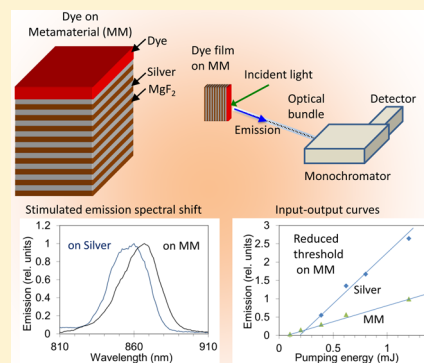
# Stimulated Emission of Surface Plasmons on Top of Metamaterials with Hyperbolic Dispersion

John K. Kitur, Lei Gu, Thejaswi Tumkur, Carl Bonner, and Mikhail A. Noginov\*

Center for Materials Research, Norfolk State University, Norfolk, Virginia 23504, United States

**ABSTRACT:** We have demonstrated that the stimulated emission of surface plasmons propagating on top of multilayered hyperbolic metamaterials coated with dye-doped polymeric films has a much lower (2.5–7 times) threshold than that on top of thick Ag films. This observation correlates with more than 2-fold shortening of the spontaneous emission kinetics on top of a lamellar metamaterial as compared to that on top of silver. The propagation of surface plasmons on top of the metamaterial and silver substrates was modeled (in the Otto geometry) using COMSOL Multiphysics. It has been shown that at given system parameters, the plasmon propagation loss in a metamaterial is smaller than that in silver by  $\sim 14\%$  and cannot explain the dramatic reduction of the lasing threshold observed experimentally in the metamaterial samples. We infer that the stimulated emission of propagating plasmons on top of a metamaterial is enhanced by the nonlocal dielectric environment and high local density of photonic states.

**KEYWORDS:** metamaterials, surface plasmons, stimulated emission



Localized surface plasmons (SPs; oscillations of free electron density in metallic nanostructures<sup>1–3</sup>) and propagating SPs (the most widely known of which are surface plasmon polaritons, SPPs, electromagnetic surface waves propagating at the interface between metal and dielectric<sup>3–6</sup>) determine the research field of plasmonics. They play a key role in a variety of sensors,<sup>7–9</sup> medical diagnostics<sup>10</sup> and treatments,<sup>11</sup> communication and information technologies,<sup>12,13</sup> and photovoltaic devices.<sup>14,15</sup> (Here by “metal” we mean any medium with negative real part of dielectric permittivity.) Surface plasmons have enabled unparalleled properties of many metamaterials—engineered artificial media comprised of sub-wavelength inclusions, “meta-atoms”, with custom tailored sizes, shapes, mutual orientations, and compositions, embedded in a host matrix.<sup>16</sup> Fascinating theoretical predictions and experimental demonstrations of metamaterials include invisibility cloaking,<sup>17,18</sup> negative index of refraction,<sup>19–21</sup> subdiffraction focusing and imaging,<sup>17,22–24</sup> as well as table-top modeling of cosmological phenomena.<sup>25,26</sup>

Most of the existing metamaterials and plasmonic devices are passive. However, novel designs and concepts, such as future electronics operating at optical frequencies,<sup>27</sup> call for active materials and systems with nonlinearity,<sup>28–30</sup> optical gain,<sup>31,32</sup> and tunability.<sup>33–35</sup> On the other hand, optical loss in the metal presents a substantial challenge to the widespread use of metamaterials and plasmonics. The losses can be compensated by optical gain in an adjacent dielectric.<sup>28,36–38</sup> If the gain overcomes absorption loss in metal, stimulated emission of SPs occurs. This effect has been theoretically predicted and experimentally demonstrated for both localized<sup>29,39,40</sup> and propagating<sup>28,41–43</sup> surface plasmons.

In our earlier studies,<sup>41–43</sup> stimulated emission of surface plasmon polaritons has been demonstrated at visible wave-

lengths using rhodamine 6G and rhodamine B laser dyes. However, the required high optical gain ( $\geq 1000 \text{ cm}^{-1}$ ) made this phenomenon impractical. At the same time, the lasing threshold can be reduced by more than 20 times<sup>44</sup> in the near-infrared range of the spectrum, where the absorption loss of SPPs is relatively low and the highly efficient HITC laser dye is available.

In search for a further reduction of the lasing threshold of propagating surface plasmons, we have turned our attention to lamellar metal/dielectric structures, which can support a variety of SP modes.<sup>45–49</sup> In materials with such morphology, described in an effective medium approximation, real parts of dielectric permittivities in orthogonal directions can have opposite signs, and isofrequency dispersion surfaces for extraordinary waves can be hyperboloids instead of more conventional spheres or ellipsoids.<sup>22,50,51</sup> The latter phenomenon determines the name “hyperbolic metamaterial”.<sup>22</sup> It also results in a very high local density of photonic states inside hyperbolic metamaterials and in the vicinity of their surfaces.<sup>52</sup> In accord with the Fermi’s Golden Rule, the broad-band singularity and anisotropy of the photonic density of states increase the rate and change the directionality of spontaneous emission<sup>53–56</sup> as well as result in a dramatic reduction of reflection from roughened hyperbolic metamaterials.<sup>57,58</sup>

The literature has multiple reports attributing the high density of states in photonic crystals, which coexists with the slow group velocity, to an increase in the optical gain and reduction in the stimulated emission threshold in amplifiers and lasers.<sup>59–62</sup> This claim, which has been confirmed experimen-

Received: December 21, 2014

Published: July 9, 2015

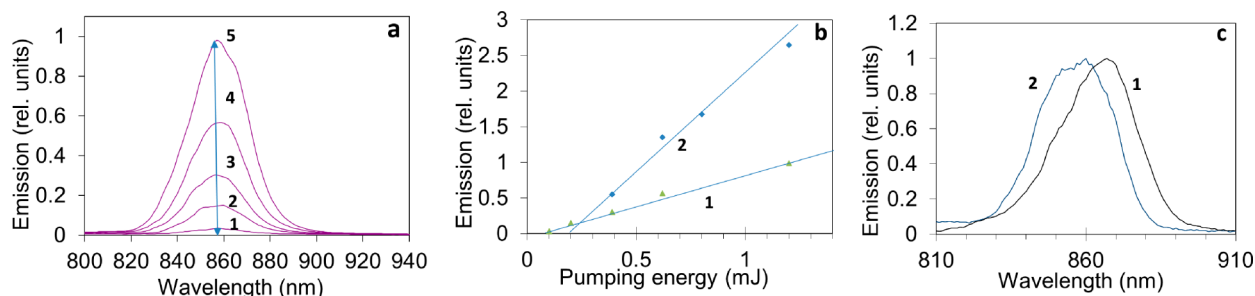


**Figure 1.** (a) Spectra of stimulated emission of the  $200 \pm 10$  nm HITC-doped PMMA film on top of lamellar metamaterial at the pumping energy equal to 0.1 (1), 0.2 (2), 0.39 (3), 0.62 (4), and 1.2 mJ (5). (b) Input–output dependences for the  $200 \pm 10$  nm HITC-doped PMMA film on top of lamellar metamaterial (1) and Ag (2). (c) Spectra of stimulated emission of the  $200 \pm 10$  nm HITC-doped PMMA film on top of lamellar metamaterial (1) and Ag (2).

tally in photonic crystals and waveguides,<sup>59,62</sup> agrees with the Fermi's Golden Rule (postulating the transition rate is proportional to the final density of states), when a relatively broad spectral band of stimulated emission or amplified spontaneous emission overlaps with multiple photonic modes. These reports and the underlying reasoning have motivated us to study the stimulated emission of propagating surface plasmons on top of multilayered metal/dielectric metamaterials with hyperbolic dispersion.

The nature of the plasmon propagation on top of multilayered metal/dielectric structures requires some special attention. It has been shown<sup>45,48,49</sup> that these plasmons are not the familiar SPPs residing at the interface of the outmost metallic layer and air, but rather a family of bulk plasmons comprised of multiply coupled (to each other) gap plasmons supported by metal-dielectric-metal triads of the multilayered metamaterial. Therefore, the plasmon propagation loss in lamellar multilayers can be different from that of SPPs on top of thick metallic films. If the propagation loss of a bulk plasmon is smaller than that of the SPP, the lasing threshold can be reduced even further. (Below, unless we need to emphasize the complex structure of these bulk plasmons, we will refer to them as surface plasmons.)

## MATERIALS AND METHODS

**Fabrication and Characterization of the Metamaterial Samples.** Lamellar metamaterials, fabricated on glass substrates using thermal vapor deposition technique (Nano 36 from Kurt J. Lesker), consisted of six 35 nm  $\text{MgF}_2$  layers and six 25 nm Ag layers (Ag on top). In order to evaluate their effective permittivities in the directions parallel  $\epsilon_{\parallel}$  and perpendicular  $\epsilon_{\perp}$  to the layers, we have measured the dependence of the  $p$ -polarized and  $s$ -polarized reflectance on the incidence angle,  $R(\theta)$ , and fitted the experimental data with the known equations.<sup>63</sup> At the wavelength  $\lambda = 860$  nm, the dielectric permittivities were found to be  $\epsilon_{\parallel} = -5.8 + i1.2$  and  $\epsilon_{\perp} = -1.4 + i0.03$ , and correspondingly, the metamaterials had a hyperbolic dispersion. Thick silver films ( $\sim 200 \pm 10$  nm), deposited onto glass substrates, served as control samples.

**Deposition of the Polymeric Films.** The HITC laser dye (2-[7-(1,3-dihydro-1,3,3-trimethyl-2H-indol-2-ylidene)-1,3,5-heptatrienyl]-1,3,3-trimethyl-3H-indolium iodide) doped into poly(methyl methacrylate) (PMMA) polymer in concentration 20 g/L (40 mM) was spin-coated on the lamellar metamaterial and control samples (Spin-Coater Model P6700 from Specialty Coating Systems). The thickness of the polymeric films was

equal to  $200 \pm 10$  nm. (All thickness measurements were done with the Dektak XT profilometer from Bruker.)

**Laser Pumping and Emission Measurements.** The dyedoped polymeric films were excited at the wavelength  $\lambda = 750$  nm and the incidence angle  $\theta = 90^\circ$  with 5 ns pulses from an optical parametric oscillator (Panther EX PLUS pumped by Surelight SLIII from Continuum). The pumped spot diameter, determined using the knife-edge technique, was 1.7 mm. The emission from the sample was collected at  $\sim 45^\circ$  and directed to the monochromator (MS 257 from Newport/Oriel) equipped with Hamamatsu R2658 photomultiplier detector attached to the exit slit of the monochromator. Emission spectra were collected at optical pumping densities ranging from 7.0 to 225  $\text{J}/\text{cm}^2$ .

**Spontaneous Emission Kinetics.** In the spontaneous emission kinetics measurements, the samples were excited at  $\lambda = 760$  nm with the 200 fs Ti:sapphire laser (Mira 900 pumped with 28W Innova Ar+ laser from Coherent). The repetition rate was 76 MHz. The average power on the sample was equal to 19.3 mW, and the pumped spot diameter was approximately equal to 0.15 mm. The emission kinetics were measured using the near-infrared streak camera from Hamamatsu (model C5680). Proper long-pass filters installed in front of the streak camera were used to block the pumping light and transmit the spontaneous emission. The response time of the apparatus, determined by the wide-open slits of the streak camera and jitter of the laser, was equal to 80 ps.

## RESULTS AND DISCUSSION

**Stimulated Emission Studies.** At low pumping intensity, only the spontaneous emission band was observed in the spectrum at  $\lambda \sim 810$  nm (not seen in the scale of Figure 1a). With an increase of the pumping energy, a second spectral band appeared at  $\lambda \sim 860$  nm, Figure 1a. Following refs 41, 43, and 44, this band is attributed to stimulated emission of surface (or bulk) plasmons without intentional feedback. As the pumping intensity was increased further, the stimulated emission band also grew, as shown in Figure 1a.

The intensity of stimulated emission from the HITC-doped PMMA films on top of lamellar metamaterial and the silver film (measured as shown by the arrow in Figure 1a) has been plotted against the pumping energy to comprise the input–output stimulated emission curves, Figure 1b.

Three sets of nominally identical metamaterial and silver samples were fabricated and three sets of identical measurements have been carried out independently from each other. In all experimental trials, both the threshold pumping energy  $E_{\text{in}}^{\text{th}}$

and the slope efficiency,  $dE_{\text{out}}/dE_{\text{in}}$ , were much smaller in dye/polymer films on the metamaterial (MM) than on silver (see Figure 1b showing the results of one representative experiment). To be more specific, the three ratios of the stimulated emission thresholds ( $(E_{\text{in}}^{\text{th}})^{\text{MM}}/(E_{\text{in}}^{\text{th}})^{\text{Ag}}$ ) were equal to  $0.14 \pm 0.05$ ,  $0.23 \pm 0.05$ , and  $0.40 \pm 0.05$ , and the corresponding ratios of the slope efficiencies ( $(dE_{\text{out}}/dE_{\text{in}})^{\text{MM}}/(dE_{\text{out}}/dE_{\text{in}})^{\text{Ag}}$ ) were equal to  $0.32 \pm 0.05$ ,  $0.35 \pm 0.05$ , and  $0.32 \pm 0.05$ .

Of particular note is a red shift of stimulated emission measured on top of a metamaterial relative to that on top of Ag film (Figure 1c). In tunable lasers featuring partly overlapping absorption and emission bands, such a red shift is indicative of a lower loss in the system.<sup>44</sup> In our experiments, this indication of a lower loss qualitatively correlates with the reduction of the lasing threshold in the metamaterial sample.

To confirm the effect of our metamaterial on the spontaneous emission, we split one of the lamellar metamaterials samples in two. Onto one side, we deposited the polymeric film heavily doped with the HITC dye (20 g/L) and used it to measure the reduction of the lasing threshold, which in the case of this particular sample was equal to  $((E_{\text{in}}^{\text{th}})^{\text{MM}}/(E_{\text{in}}^{\text{th}})^{\text{Ag}}) = 0.23$ . Onto the other half of the same sample (as well as Ag and glass substrates), we have deposited the polymeric film doped with the same dye in much smaller concentration (3 g/L) and studied its spontaneous emission kinetics. The PMMA film thickness in this particular experiment was equal to  $80 \pm 5$  nm. The small concentration of the HiTC dye was chosen to minimize concentration quenching.

The normalized emission decay kinetics  $I(t)$  of the HITC-doped PMMA films deposited onto the metamaterial, silver, and glass are depicted in Figure 2. In agreement with multiple

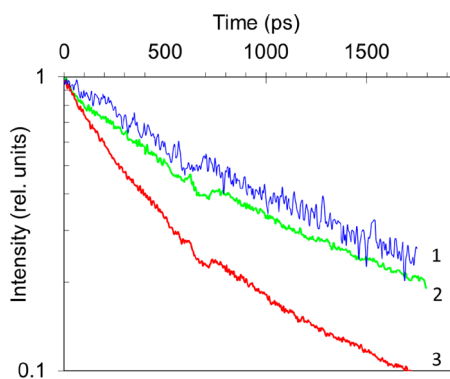


**Figure 2.** Spontaneous emission kinetics of HITC-doped PMMA films (3 g/L) measured on top of glass (1), silver (2), and metamaterial (3).

reports,<sup>53–56</sup> the emission lifetime in the metamaterial sample,  $\tau$ , defined as  $\int_0^{t_{\text{max}}} e^{-t/\tau} = \int_0^{t_{\text{max}}} I(t)(dt/I_0)$ , was much shorter than those in the Ag and glass substrate samples, Figure 2. (Here,  $I_0$  is the maximal emission intensity measured immediately after the pumping pulse, and  $t_{\text{max}}$  is the duration of the recorded emission kinetics determined by the maximal limit of the streak camera.) The reduction of the emission lifetime is characteristic feature of the high photonic density of states in a metamaterial with hyperbolic dispersion.<sup>52</sup> Note, the ratio  $\tau_{\text{MM}}/\tau_{\text{Ag}}$  was equal to  $0.43 \pm 0.05$ , larger than the ratio of the stimulated emission thresholds ( $(E_{\text{in}}^{\text{th}})^{\text{MM}}/(E_{\text{in}}^{\text{th}})^{\text{Ag}} = 0.23 \pm 0.05$ , and reasonably close to the ratio of the slope efficiencies,  $((dE_{\text{out}}/dE_{\text{in}})^{\text{MM}}/(dE_{\text{out}}/dE_{\text{in}})^{\text{Ag}}) = 0.35 \pm 0.05$ .

An alternate cause for the observed reduction of the stimulated emission threshold on top of hyperbolic meta-

material, might be a reduced internal loss of the plasmon propagation. To investigate this possibility, we modeled the system using the COMSOL Multiphysics software package. We chose to simulate plasmons excited in the Otto configuration<sup>6</sup> (Figure 3a), since it allows to efficiently excite plasmons in the top layers of the metamaterial, which are close to the dye-doped polymeric film.

Our system consisted of the following layers, from top to bottom: (i) glass with the high refractive index  $n = 1.8$  ( $2 \mu\text{m}$  thick), (ii) PMMA layer ( $n = 1.5$ , varied thickness), (iii) lamellar metamaterial consisting of seven layers of Ag ( $\epsilon_{i=860\text{nm}} = -36.74 + i0.49$ ,<sup>64</sup> 25 nm thick) and six layers of  $\text{MgF}_2$  ( $n = 1.374$ , 35 nm thick), and (iv) lower index glass ( $n = 1.5$ ,  $1 \mu\text{m}$  thick), see Figure Figure 3a. This structure was sandwiched from the top and from the bottom between the nonreflecting perfect matching layers (PMLs). The periodic boundary condition was chosen on the left and right vertical walls, and an appropriate mesh size (much smaller than the thickness of the thinnest layer in the system) has been selected. In a simulated control sample, the lamellar metamaterial was replaced with the single 600 nm Ag layer, Figure 3b.

The system was excited from the top (at  $\lambda = 860$  nm) by the TM polarized plane wave, whose angle of incidence varied between  $\theta = 30$  and  $80^\circ$ . In our study, we modeled both the electric field distribution ( $y$  component, Figure 3a,b) and the angular reflectance profile  $R(\theta)$  (Figure 3c). The width of the characteristic dip in the angular reflectance profile (Figure 3c) has been used as the measure of the plasmon's loss, which has both the radiative and the propagation (absorption) components.<sup>38</sup> The radiative loss decreases with increasing thickness of the low index spacer  $d$  (PMMA layer), while the propagation loss is independent of spacer layer thickness,  $d$ .<sup>4</sup> The full width at half-maximum (fwhm) of the angular reflectance profile  $\Delta\theta$  is depicted in Figure 3d for metamaterial and silver as the function of the spacer thickness  $d$ . As expected,  $\Delta\theta$  decreased with an increase of  $d$  at small thicknesses of the spacer and saturated at  $d > 1200$  nm, where the propagation loss dominated over the radiative loss. In the latter range of large spacer thicknesses, the surface plasmon propagation loss in the metamaterial was only marginally smaller (by  $\sim 14\%$ ) than that in silver. This difference is too small to explain the 2-fold-to-7-fold reduction of the lasing threshold observed on top of hyperbolic metamaterial substrates.

One can argue that the same high photonic density of states (which in photonic crystals is closely related to the reduced group velocity) should increase the absorption loss in metal, which, in turn, will compensate the enhancement of gain, leading to no change in the stimulated emission threshold.<sup>59,61</sup> To address this hypothetical argument, we note that, although the group velocity is related to the density of photonic states, these are two distinctly different phenomena. Thus, according to ref 65, the absorption is affected by the speed of light in the medium but is not directly influenced by the photonic density of states. This statement is in line with the results of the recent study,<sup>66</sup> showing that the dispersion of the Purcell factor in hyperbolic metamaterials strongly influences the spontaneous emission spectra but not the excitation spectra. Furthermore, absorption is not the only loss mechanism determining the stimulated emission threshold in the system. Other factors include out-of-plane decoupling (allowing us to detect the stimulated emission) and possible unintentional feedback originating from inhomogeneous film thickness or surface roughness.<sup>43</sup> If the radiative losses are strong, then enhance-



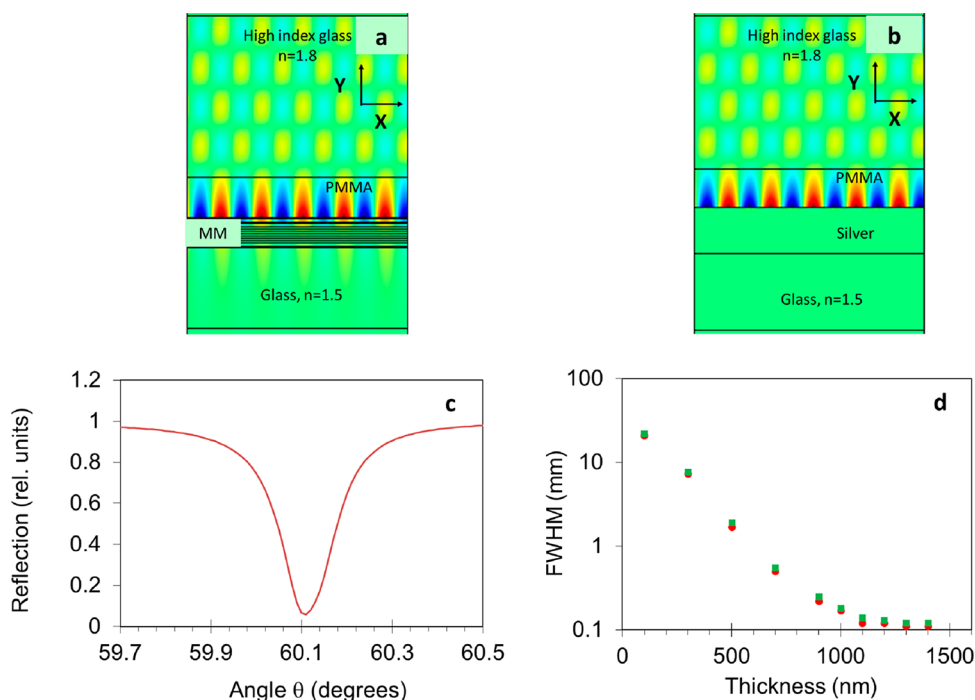


**Figure 3.** COMSOL simulation of propagating plasmons on top of lamellar hyperbolic metamaterial (a) and silver (b) in the Otto configuration. Angular reflectance profile  $\Delta\theta$  calculated for the lamellar metamaterial with the  $d = 1100$  nm spacer (PMMA) on top (c). Width of the dip in the angular reflectance profile  $\Delta\theta$  (proportional to the total plasmon loss), plotted as a function of the spacer thickness  $d$ ; silver (green squares), metamaterial (red circles).

ment of the optical gain by the high photonic density of states should reduce the threshold, as it happens in nearly lossless dielectric photonic crystals,<sup>59,61</sup> and any hypothetical changes of absorption become unimportant.

## CONCLUSIONS

We have shown that the stimulated emission of surface plasmons propagating on top of multilayered metal/dielectric hyperbolic metamaterials coated with optically pumped dye-doped polymer has a much lower (nearly 3-fold to 7-fold) threshold than that in similar films coated on top of thick Ag films. The corresponding slope efficiency for dye-doped polymer films on the metamaterial samples is 3-fold smaller than that in similar films on the silver substrates. These observations correlate with greater than 2-fold shortening of spontaneous emission lifetime from films on the metamaterial as compared to those on top of Ag. The propagation of surface plasmons on top of lamellar metamaterials and Ag substrates (excited in the Otto geometry) was modeled with COMSOL Multiphysics. It has been shown that, at the given system parameters, the internal plasmon loss of SPP in the metamaterial is smaller than that in silver by  $\sim 14\%$ , and this small difference cannot explain dramatic reduction of the lasing threshold observed experimentally. This prompts us to conclude that the stimulated emission of propagating plasmons on top of the metamaterial is, indeed, enhanced by the nonlocal dielectric environment and high local density of photonic states. The reported experimental results pave the way to active plasmonics and bring it closer to reality.

## AUTHOR INFORMATION

### Corresponding Author

\*E-mail: mnoginov@nsu.edu.

## Notes

The authors declare no competing financial interest.

## ACKNOWLEDGMENTS

The authors acknowledge NSF IGERT Grant DGE 0966188, ARO Grant W911NF-14-1-0639, FA9550-14-1-0221, NSF RISE Grant HRD-1345215, and NSF PREM Grant DMR 1205457.

## REFERENCES

- (1) Ritchie, R. Surface plasmons in solids. *Surf. Sci.* **1973**, *34*, 1–19.
- (2) Moskovits, M. Surface-enhanced spectroscopy. *Rev. Mod. Phys.* **1985**, *57* (3), 783.
- (3) Maier, S. *Plasmonics: Fundamentals and Applications*; Springer: New York, 2010.
- (4) Raether, H. *Surface Plasmons on Smooth and Rough Surfaces and on Gratings*, 1st ed.; Springer-Verlag: Berlin, 1988.
- (5) Kretschmann, E.; Raether, H. Radiative decay of non-radiative surface plasmons excited by light (Surface plasma waves excitation by light and decay into photons applied to nonradiative modes). *Z. Naturforsch., A: Phys. Sci.* **1968**, *23*, 2135.
- (6) Otto, A. Excitation Of Nonradiative Surface Plasma Waves In Silver By The Method Of Frustrated Total Reflection. *Eur. Phys. J. A* **1968**, *216*, 398–410.
- (7) Kneipp, K.; Moskovits, M.; Kneipp, H. *Surface-Enhanced Raman Scattering*; Springer: Berlin, 2006.
- (8) Anker, J.; Hall, W.; Lyandres, O.; Shah, N.; Zhao, J.; Van Duyne, R. Biosensing with Plasmonic Nanosensors. *Nat. Mater.* **2008**, *7*, 442–453.
- (9) Aslan, K.; Lakowicz, J.; Geddes, C. Nanogold Plasmon Resonance-Based Glucose Sensing. 2. Wavelength-Ratiometric Resonance Light Scattering. *Anal. Chem.* **2005**, *77*, 2007–2014.
- (10) El-Sayed, I.; Huang, X.; El-Sayed, M. Surface Plasmon Resonance Scattering And Absorption Of Anti-EGFR Antibody Conjugated Gold Nanoparticles In Cancer Diagnostics: Applications In Oral Cancer. *Nano Lett.* **2005**, *5*, 829–834.

- (11) Hirsch, L.; Stafford, R.; Bankson, J.; Sershen, S.; Rivera, B.; Price, R.; Hazle, J.; Halas, N.; West, J. Nanoshell-Mediated Near-Infrared Thermal Therapy Of Tumors Under Magnetic Resonance Guidance. *Proc. Natl. Acad. Sci. U. S. A.* **2003**, *100*, 13549–13554.
- (12) Bozhevolnyi, S.; Volkov, V.; Devaux, E.; Laluet, J.; Ebbesen, T. Channel Plasmon Subwavelength Waveguide Components Including Interferometers And Ring Resonators. *Nature* **2006**, *440*, 508–511.
- (13) Atwater, H. The Promise Of plasmonics. *Scientific American* **2007**, *17*, 56–63.
- (14) Atwater, H.; Polman, A. Plasmonics for Improved Photovoltaic Devices. *Nat. Mater.* **2010**, *9*, 205–213.
- (15) Pala, R.; White, J.; Barnard, E.; Liu, J.; Brongersma, M. Design Of Plasmonic Thin-Film Solar Cells With Broadband Absorption Enhancements. *Adv. Mater.* **2009**, *21*, 3504–3509.
- (16) Noginov, M.; Podolskiy, V. *Tutorials in Metamaterials*; Taylor & Francis: Boca Raton, FL, 2012.
- (17) Pendry, J.; Schurig, D.; Smith, D. Controlling Electromagnetic Fields. *Science* **2006**, *312*, 1780–1782.
- (18) Cai, W.; Chettiar, U.; Kildishev, A.; Shalaev, V. Optical Cloaking With Metamaterials. *Nat. Photonics* **2007**, *1*, 224–227.
- (19) Pendry, J. Negative Refraction Makes A Perfect Lens. *Phys. Rev. Lett.* **2000**, *85*, 3966–3969.
- (20) Shelby, R. Experimental Verification of A Negative Index Of Refraction. *Science* **2001**, *292*, 77–79.
- (21) Shalaev, V.; Cai, W.; Chettiar, U.; Yuan, H.; Sarychev, A.; Drachev, V.; Kildishev, A. Negative Index Of Refraction In Optical Metamaterials. *Opt. Lett.* **2005**, *30*, 3356.
- (22) Jacob, Z.; Alekseyev, L.; Narimanov, E. Optical Hyperlens: Far-Field Imaging Beyond the Diffraction Limit. *Opt. Express* **2006**, *14*, 8247.
- (23) Salandrino, A.; Engheta, N. Far-Field Subdiffraction Optical Microscopy Using Metamaterial Crystals: Theory and Simulations. *Phys. Rev. B: Condens. Matter Mater. Phys.* **2006**, *74* (7), 075103.
- (24) Liu, Z.; Lee, H.; Xiong, Y.; Sun, C.; Zhang, X. Far-Field Optical Hyperlens Magnifying Sub-Diffraction-Limited Objects. *Science* **2007**, *315*, 1686–1686.
- (25) Smolyaninov, I.; Narimanov, E. Metric Signature Transitions in Optical Metamaterials. *Phys. Rev. Lett.* **2010**, *105*, 067402.
- (26) Smolyaninov, I.; Hung, Y.; Hwang, E. Experimental Modeling of Cosmological Inflation with Metamaterials. *Phys. Lett. A* **2012**, *376*, 2575–2579.
- (27) Engheta, N. Circuits With Light At Nanoscales: Optical Nanocircuits Inspired By Metamaterials. *Science* **2007**, *317*, 1698–1702.
- (28) Kauranen, M.; Zayats, A. Nonlinear Plasmonics. *Nat. Photonics* **2012**, *6*, 737–748.
- (29) Liu, Y.; Bartal, G.; Genov, D.; Zhang, X. Subwavelength Discrete Solitons in Nonlinear Metamaterials. *Phys. Rev. Lett.* **2007**, *99*, 153901.
- (30) Shadrivov, I.; Kozyrev, A.; van der Weide, D.; Kivshar, Y. Tunable Transmission and Harmonic Generation in Nonlinear Metamaterials. *Appl. Phys. Lett.* **2008**, *93*, 161903.
- (31) Sudarkin, A.; Demkovich, P. Excitation of surface electromagnetic waves on the boundary of a metal with an amplifying medium. *Sov. Phys. Tech. Phys.* **1989**, *34*, 764–766.
- (32) Bergman, D.; Stockman, M. Surface Plasmon Amplification by Stimulated Emission of Radiation: Quantum Generation of Coherent Surface Plasmons in Nanosystems. *Phys. Rev. Lett.* **2003**, *90*, 10.1103/PhysRevLett.90.027402.
- (33) Xiao, S.; Chettiar, U.; Kildishev, A.; Drachev, V.; Khoo, I.; Shalaev, V. Tunable Magnetic Response of Metamaterials. *Appl. Phys. Lett.* **2009**, *95*, 033115.
- (34) Dicken, M.; Aydin, K.; Pryce, I.; Sweatlock, L.; Boyd, E.; Walavalkar, S.; Ma, J.; Atwater, H. Frequency Tunable Near-Infrared Metamaterials Based On VO<sub>2</sub> Phase Transition. *Opt. Express* **2009**, *17*, 18330.
- (35) Ou, J.; Plum, E.; Zhang, J.; Zheludev, N. An Electromechanically Reconfigurable Plasmonic Metamaterial Operating In The Near-Infrared. *Nat. Nanotechnol.* **2013**, *8*, 252–255.
- (36) Lawandy, N. Localized Surface Plasmon Singularities In Amplifying Media. *Appl. Phys. Lett.* **2004**, *85*, 5040.
- (37) Seidel, J.; Grafstrom, S.; Eng, L. Stimulated Emission of Surface Plasmons at the Interface between A Silver Film and an Optically Pumped Dye Solution. *Phys. Rev. Lett.* **2005**, *94*, 10.1103/PhysRevLett.94.177401.
- (38) Noginov, M.; Podolskiy, V.; Zhu, G.; Mayy, M.; Bahoura, M.; Adegoke, J.; Ritzo, B.; Reynolds, K. Compensation Of Loss In Propagating Surface Plasmon Polariton By Gain In Adjacent Dielectric Medium. *Opt. Express* **2008**, *16*, 1385.
- (39) Noginov, M.; Zhu, G.; Belgrave, A.; Bakker, R.; Shalaev, V.; Narimanov, E.; Stout, S.; Herz, E.; Suteewong, T.; Wiesner, U. Demonstration of A Spaser-Based Nanolaser. *Nature* **2009**, *460*, 1110–1112.
- (40) Oulton, R.; Sorger, V.; Zentgraf, T.; Ma, R.; Gladden, C.; Dai, L.; Bartal, G.; Zhang, X. Plasmon Lasers at Deep Subwavelength Scale. *Nature* **2009**, *461*, 629–632.
- (41) Noginov, M.; Zhu, G.; Mayy, M.; Ritzo, B.; Noginova, N.; Podolskiy, V. Stimulated Emission of Surface Plasmon Polaritons. *Phys. Rev. Lett.* **2008**, *101*, 226806.
- (42) Kitur, J.; Podolskiy, V.; Noginov, M. Stimulated Emission of Surface Plasmon Polaritons in A Microcylinder Cavity. *Phys. Rev. Lett.* **2011**, *106*, 183903.
- (43) Kitur, J.; Zhu, G.; Barnakov, Y.; Noginov, M. Stimulated Emission of Surface Plasmon Polaritons on Smooth and Corrugated Silver Surfaces. *J. Opt.* **2012**, *14*, 114015.
- (44) Kitur, J.; Zhu, G.; Noginov, M. Low-Threshold Stimulated Emission of Surface Plasmons Polaritons. *J. Opt.* **2014**, *16*, 114020.
- (45) Avrutsky, I.; Salakhutdinov, I.; Elser, J.; Podolskiy, V. Highly Confined Optical Modes in Nanoscale Metal-Dielectric Multilayers. *Phys. Rev. B: Condens. Matter Mater. Phys.* **2007**, *75*, 241402(R).
- (46) Sreekanth, K.; De Luca, A.; Strangi, G. Experimental Demonstration of Surface and Bulk Plasmon Polaritons in Hypergratings. *Sci. Rep.* **2013**, *3*, 10.1038/srep03291.
- (47) Vukovic, S.; Shadrivov, I.; Kivshar, Y. Surface Bloch Waves in Metamaterial and Metal-Dielectric Superlattices. *Appl. Phys. Lett.* **2009**, *95*, 041902.
- (48) Nam, S.; Ulin-Avila, E.; Bartal, G.; Zhang, X. General Properties of Surface Modes in Binary Metal-Dielectric Metamaterials. *Opt. Express* **2010**, *18*, 25627.
- (49) Hyun Nam, S.; Ulin-Avila, E.; Bartal, G.; Zhang, X. Deep Subwavelength Surface Modes in Metal-Dielectric Metamaterials. *Opt. Lett.* **2010**, *35*, 1847.
- (50) Smith, D.; Schurig, D. Electromagnetic Wave Propagation in Media with Indefinite Permittivity and Permeability Tensors. *Phys. Rev. Lett.* **2003**, *90*, 077405.
- (51) Belov, P.; Marques, R.; Maslovski, S.; Nefedov, I.; Silveirinha, M.; Simovski, C.; Tretyakov, S. Strong Spatial Dispersion in Wire Media in the Very Large Wavelength Limit. *Phys. Rev. B: Condens. Matter Mater. Phys.* **2003**, *67*, 113103.
- (52) Jacob, Z.; Smolyaninov, I.; Narimanov, E. Broadband Purcell Effect: Radiative Decay Engineering with Metamaterials. *Appl. Phys. Lett.* **2012**, *100*, 181105.
- (53) Noginov, M.; Li, H.; Barnakov, Y.; Dryden, D.; Nataraj, G.; Zhu, G.; Bonner, C.; Mayy, M.; Jacob, Z.; Narimanov, E. Controlling Spontaneous Emission With Metamaterials. *Opt. Lett.* **2010**, *35*, 1863.
- (54) Jacob, Z.; Kim, J.; Naik, G.; Boltasseva, A.; Narimanov, E.; Shalaev, V. Engineering Photonic Density Of States Using Metamaterials. *Appl. Phys. B: Lasers Opt.* **2010**, *100*, 215–218.
- (55) Tumkur, T.; Zhu, G.; Black, P.; Barnakov, Y.; Bonner, C.; Noginov, M. Control Of Spontaneous Emission In A Volume Of Functionalized Hyperbolic Metamaterial. *Appl. Phys. Lett.* **2011**, *99*, 151115.
- (56) Krishnamoorthy, H.; Jacob, Z.; Narimanov, E.; Kretzschmar, I.; Menon, V. Topological Transitions in Metamaterials. *Science* **2012**, *336*, 205–209.
- (57) Narimanov, E.; Li, H.; Barnakov, Y.; Tumkur, T.; Noginov, M. Reduced Reflection From Roughened Hyperbolic Metamaterial. *Opt. Express* **2013**, *21*, 14956.

(58) Tumkur, T.; Kitur, J.; Chu, B.; Gu, L.; Podolskiy, V.; Narimanov, E.; Noginov, M. Control Of Reflectance And Transmittance In Scattering And Curvilinear Hyperbolic Metamaterials. *Appl. Phys. Lett.* **2012**, *101*, 091105.

(59) Ek, S.; Lunnemann, P.; Chen, Y.; Semenova, E.; Yvind, K.; Mork, J. Slow-Light-Enhanced Gain In Active Photonic Crystal Waveguides. *Nat. Commun.* **2014**, *5*, 5039.

(60) Dowling, J.; Scalora, M.; Bloemer, M.; Bowden, C. The Photonic Band Edge Laser: A New Approach to Gain Enhancement. *J. Appl. Phys.* **1994**, *75*, 1896.

(61) Sakoda, K. *Optical Properties of Photonic Crystals*; Springer: Heidelberg, 2001.

(62) Sapienza, R.; Leonetti, M.; Froufe-Perez, L.; Galisteo-Lopez, J.; Conti, C.; Lopez, C. Optical Amplification Enhancement in Photonic Crystals. *Phys. Rev. A: At., Mol., Opt. Phys.* **2011**, *83*, 023801.

(63) Noginov, M.; Barnakov, Y.; Zhu, G.; Tumkur, T.; Li, H.; Narimanov, E. Bulk Photonic Metamaterial With Hyperbolic Dispersion. *Appl. Phys. Lett.* **2009**, *94*, 151105.

(64) Johnson, P.; Christy, R. Optical Constants of the Noble Metals. *Phys. Rev. B* **1972**, *6*, 4370–4379.

(65) Pantell, R. Theoretical and Experimental Values for Two-, Three-, and Four-Photon Absorptions. *J. Chem. Phys.* **1967**, *46*, 3507.

(66) Gu, L.; Livenere, J.; Zhu, G.; Tumkur, T.; Hu, H.; Cortes, C.; Jacob, Z.; Prokes, S.; Noginov, M. Angular Distribution Of Emission From Hyperbolic Metamaterials. *Sci. Rep.* **2014**, *4*, 7327.